RADIATION DAMAGE EFFECT ON STRUCTURAL AND MECHANICAL PROPERTIES OF INERT ZrN LAYER: CORROSION MITIGATION IN LBE COOLING ENVIRONMENT

M. IZERROUKEN[1], M. AZIBI[2], N. SAOULA[2], F. HAID[2], A. SARI[3], A. ISHAQ[4]

[1]Nuclear Research Center of Draria, Bp. 43 Sebbala, Draria, Algiers, Algeria.
[2]Development Centre of Advanced Technologies, 20 August city 1956, Bp. 17, Baba Hassen, Algiers, Algeria
[3]Nuclear research center of Birine, BP 108, Ain-Oussera, Djelfa, Algeria
[4]National Center for Physics, Islamabad, 44000, Pakistan

Corresponding author: m-izerrouken@crnd.dz

Due to its multiple advantages, low thermal neutron absorption cross section, radiation damage tolerance, low melting temperature, high boiling temperature and non-reactive with air and water, Lead-Bismuth Eutectic (LBE) is a primary candidate for use as a target for the production of a spallation neutron source [1] and as the coolant for advanced nuclear reactors systems (Gen. IV) [2]. Since its development during the 1950s, extensive studies have been conducted around the world to expand the application of liquid lead and LBE technology in fast reactors cooling system. The results of most of these investigations have been discussed in the review [3]. Thermal and physical properties, coolant characteristics as well as safety issues of these cooling systems, in particular corrosion and formation of Pb-210 were also reported. Regarding corrosion issues, numerous studies revealed that the actual structural materials are destroyed in LBE environment by corrosion at high temperature under high neutron flux see review [4] and reference therein. The authors reported the latest research on the introduction of coatings on the cladding materials surface to improve the corrosion resistance in high-temperature LBE. Many coatings were experimented such as Al_2O_3, SiC, Ti_3SiC_2, TiAlN, TiSiN, amorphous Si_3N4, amorphous SiO_2 and amorphous Al_2O_3, in addition to the development of new coatings, such as amorphous High-and medium-Entropy Alloy, with high crystallization temperature, which has excellent mechanical properties and corrosion resistance. It is found that most of these coatings avoid the corrosion of different stainless steel categories (EP823, T91, HT-9, 1.4718, EP823, HCM12A, 316 L,…). Furthermore, corrosion inhibitors such as Ti and Zr have been proposed to avoid LBE corrosion. The reaction with the nitrogen and carbon of the steel container leads to the formation of protective layers ZrN, TiN, or TiN+TiC at the steel/LBE interface which inhibit corrosion [4, 5]. ZrN in particular has excellent properties that can make it a stable protective coating in the LBE environment. It is known for its high melting point, good resistance to wear, to corrosion, high mechanical properties, excellent thermal conductivity, low thermal neutron absorption cross section and high radiation tolerance [6-8]. It is interesting to note that ZrN thin film is a promising candidate as a diffusion barrier between the U-Mo fuel particles and the aluminum [9] to avoid the formation of the interaction layer $(U\text{-}Mo)Al_x$ during reactor neutron operation. It is likely that fast neutrons and charged particles from fission or fusion reactions affect the properties of the protective layer and therefore accelerate the corrosion process. Thus, theoretical and experimental studies should be carried out to identify the irradiation tolerance of such protective layers. This is the goal of the study presented in this work.

ZrN thin films elaborated using high power impulse magnetron sputtering technique were irradiated at room temperature with 2 MeV proton in a fluence range of 1×10^{13}–1×10^{15} p.cm^{-2}. The irradiations were performed at 5UDH-2 Pelletron Tandem accelerator Islamabad, Pakistan. After irradiation the defect formation was investigated using grazing incidence X-ray diffraction (GIXRD), atomic force microscopy (AFM) and nanoindentation tools.

Fig.1 depicts the GIXRD patterns of unirradiated and proton irradiated ZrN film at different fluences. The spectra show peaks at 2θ=34.6°, 39.79° and 57.29° corresponding respectively to the diffraction from 111, 200 and 220 planes of cubic lattice of ZrN film, according to the powder diffraction file (PDF) reference code 98-064-4881. The peaks assigned by star correspond to the Zr substrate. As can be seen, the intensity and position of the peaks remain unchanged after irradiation up to a fluence of 1×10^{15} p.cm^{-2}. These suggest stable crystallinity and no swelling or contraction under irradiation. Similar results have been reported earlier in ZrN film irradiated by swift heavy ions where the electronic stopping power is predominant [10, 11]. The crystallite size and the lattice strain calculated using the X'Pert High score plus software,v.2.1.0 are reported in table 1. Crystallite size and strain show a monotonic decrease and increase, respectively, above a fluence of 1×10^{14} p.cm^{-2}. This may be attributed to the nitrogen vacancies accumulation. Indeed, the nitrogen interstitials displaced by the irradiation migrate towards the grain boundaries and leave behind a cluster of vacancies which reduce the crystallite size and therefore increase the strain. Furthermore, it is worthy to note the crystallite smallness improves the corrosion resistance [12].

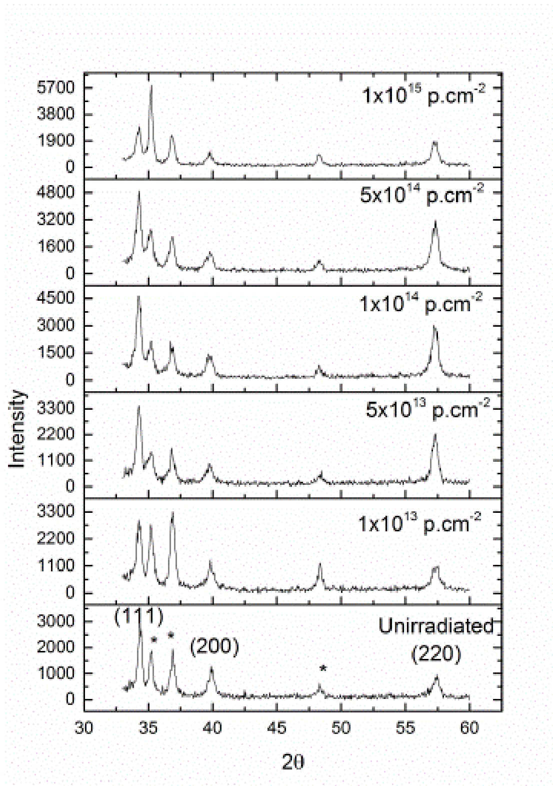

FIG.1. GIXRD spectra of ZrN film before and after 2 MeV proton irradiation at different fluences recorded at grazing incident angle of 2°.

Figs. 2a and b present the 2D images made respectively using contact mode and tapping mode on as elaborated ZrN film. The surface morphology obtained using contact-mode shows elongated grains, with a width of about 60 nm, oriented in the same direction. While the tapping-mode AFM image, in addition to the grain morphology, the picture reveals small hills on the surface of the grain. Thus, in our case, it is recommended to use tapping mode to study the roughness evolution under 2 MeV proton irradiation. Furthermore, to clearly reveal the irradiation effect on the ZrN film surface morphology, a smallest possible area of 500 nm x 500 nm was scanned. The obtained results are presented in Figs.3 a–d for unirradiated ZrN film and irradiated respectively to a fluence of 1×10^{13}, 1×10^{14}, 1×10^{15} $p.cm^{-2}$. As can be seen, the small hills observed on the grain surface of the unirradiated sample (picture a) disappear after irradiation indicating the irradiation-induced smoothening as reported in table 1 showing the value of root mean square (RMS) roughness evolution versus fluence. The RMS decreases from 5.4 nm for unirradiated sample to approximately a constant value of about 2 nm after irradiation up to a fluence of 5×10^{14} $p.cm^{-2}$. Further increasing proton fluence, the RMS decreases to 1.1±0.03 nm at 1×10^{15} $p.cm^{-2}$.

TABLE 1. THE VALUES OF CRYSTALLITE SIZE, STRAIN, RMS ROUGHNESS, HARDNESS AND YOUNG'S MODULUS VERSUS FLUENCE

Fluence ($p.cm^{-2}$)	Crystallite size (nm)	Strain (%)	RMS (nm)	Hardness (GPa)	Young's modulus (GPa)
Unirradiated	24.8±2	0.513±0.06	5.4±0.9	9.3±1.4	157±6.8
1×10^{13}	15.9±0.4	0.815±0.02	1.9±0.06	-	-
5×10^{13}	21.8±1.5	0.6±0.04	2.1±0.7	8.42±3.2	140±58
1×10^{14}	18±1	0.725±0.04	2.3±0.9	10.2±1.8	162±29
5×10^{14}	16.5±0.00	0.789±0.002	2.5±0.3	8.3±0.2	110±7.8
1×10^{15}	14.5±0.5	0.901±0.003	1.1±0.03	9.9±2.4	155±53

This smoothening may be interpreted as evaporation-condensation mechanism caused by the sputtering. This is supported by the amplitude images revealing the craters formation on the grain surface (Fig. 3) confirming the ejection of particles (sputtering) from the surface under 2 MeV proton bombardments. This is clearer from the phase AFM images indicating a difference in contrast between the crater zones and the rest of the sample (Fig.4). This difference in contrast is probably due to the difference in hardness in the two regions. While the unirradiated sample presents an almost homogeneous surface contrast. On further increasing the proton fluence, the craters density increases and overlaps, which probably explains the lower RMS value (1.1±0.03 nm) obtained at 1×10^{15} $p.cm^{-2}$. Moreover, it is known that the decreases in roughness increase the corrosion resistance [13] which makes ZrN a suitable protective coating in the LBE environment.

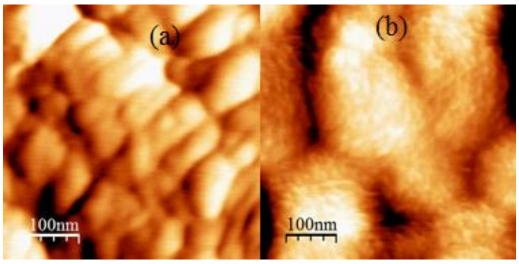

FIG. 2. 2D AFM images of as elaborated ZrN film : a- made using contact mode showing the grain morphology. b- made using tapping mode reveling small hills on the surface of the grain.

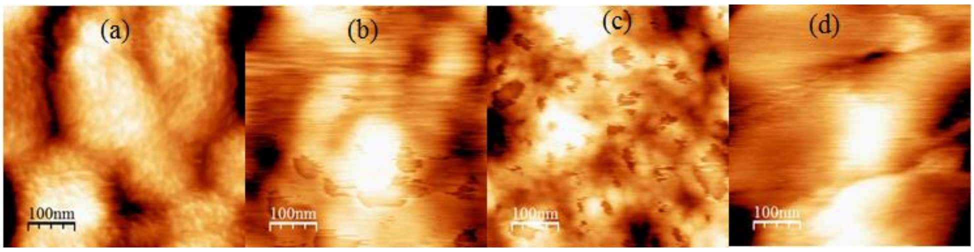

FIG. 3. Tapping-mode AFM images showing the variation of roughness of ZrN film (a) before irradiation and after irradiation by 2 MeV proton at different fluence: (b) 1×10^{13} p.cm^{-2}, (c) 1×10^{14} p.cm^{-2}, (d) 1×10^{15} p.cm^{-2}.

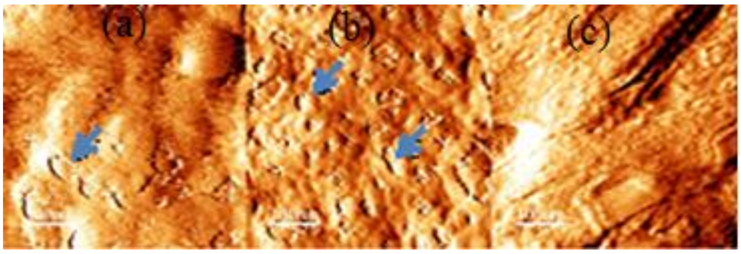

FIG. 4. Amplitude AFM images showing the formation of craters on the grains surface (indicated by blue arrow) after irradiation by 2 MeV proton at different fluence:(a) 1×10^{13} p.cm^{-2}, (b) 1×10^{14} p.cm^{-2}, (c) 1×10^{15} p.cm^{-2}.

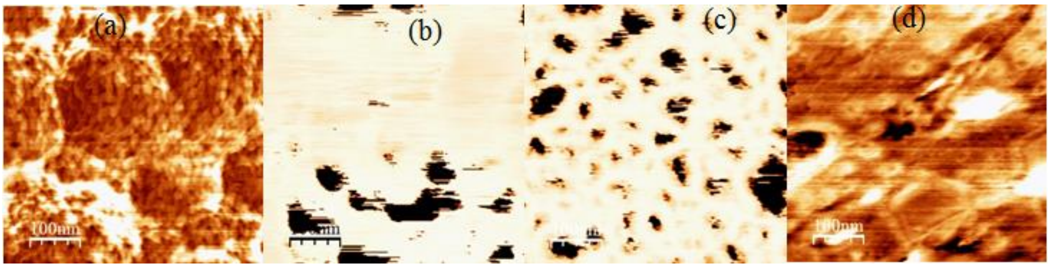

FIG. 5. Phase AFM images of (a) as elaborated ZrN film compared to the phase AFM images of the 2 MeV proton-irradiated ZrN film:(b) 1×10^{13} p.cm^{-2}, (c) 1×10^{14} p.cm^{-2}, (d) 1×10^{5} p.cm^{-2}.

The measured hardness and Young's modulus versus fluence are summarized in table 1. A large scatter is observed in the hardness and Young's modulus data as also reported by Vuuren et al. [14]. This scatter is commonly observed in shallow indentations due to many factors [15]. In our case it is due mainly to the variation in the surface morphology. The data revealed no significant changes in both hardness and Young's moduls values after irradiation in the investigated fluence range. Similar results were reported earlier indicating no appreciable effects due to radiation damage see ref. [16] and reference therein.

In summary, the present study reports the effect of 2 MeV proton irradiation on the structural, morphological and mechanical properties of ZrN film in the fluence range *1×10^{13} – 1×10^{15} p.cm^{-2}*. It is found: (a) stable crystallinity; (b) no amorphization, swelling and contraction; (c) both crystallite size and lattice strain, respectively, decrease and increase linearly with the fluence above 1×10^{14} p.cm^{-2}; (d) surface smoothening; (e) no significant change in hardness and Young's modulus. These results confirm the high radiation tolerance of the ZrN coating with strong structural stability under irradiation. Furthermore, the surface smoothening and smallness of the crystallite under irradiation improve the corrosion resistance of ZrN film.

Therefore, the ZrN protective layer formed will not be affected by irradiation, which will mitigate LBE corrosion. Thought, further investigation should be made to understand the craters formation and its effect on ZrN mechanical properties and corrosion evolution.

REFERENCES

[1] PARK, J.J., BUTT, D.P., BEARD, C.A., Review of liquid metal corrosion issues for potential +containment materials for liquid lead and lead–bismuth eutectic spallation targets as a neutron source, Nucl. Eng. and Des. 196 (2000) 315–325.

[2] POPOVIÜ, M.P. , BOLIND, A.M., CIONEA, C., HOSEMANN,P., Liquid lead-bismuth eutectic as a coolant in generation IV nuclear reactors and in high temperature solar concentrator applications: characteristics, challenges, issues, Contemp. Mater., VI-1 (2015).

[3] ZHANG, J., Lead–Bismuth Eutectic (LBE): A Coolant Candidate for Gen. IV Advanced Nuclear Reactor Concepts, Adv. Eng. Mater. 16, N° 4 (2014) 349.

[4] HAO WANG, JUN XIAO, HUI WANG, YONG CHEN, XING YIN and NING GUO, Corrosion Behavior and Surface Treatment of Cladding Materials Used in High-Temperature Lead-Bismuth Eutectic Alloy: A Review, Coatings 11 (2021) 364.

[5] ERIC P. LOEWEN, HANNAH J. YOUNT, KEVIN VOLK, ARVIND KUMAR, Layer formation on metal surfaces in lead–bismuth at high temperatures in presence of zirconium, J. of Nucl. Mater. 321 (2003) 269–280.

[6] JOHN J. PARK, DARRYL P. BUTT, CARL A. BEARD, Review of liquid metal corrosion issues for potential containment materials for liquid lead and lead–bismuth eutectic spallation targets as a neutron source, Nucl. Eng. and Design 196 (2000) 315–325.

[7] JIAO L., YU K.Y., CHEN D., JACOB C., SHAO L., ZHANG X., AND WANG H., Radiation tolerant nanocrystalline ZrN films under high dose heavy-ion Irradiations. J. of App. Phy. 117 (2015)145901.

[8] KEISER D.D., PEREZ E., WIENCEK T., LEENAERS A., VAN DEN BERGHE S., Microstructural characterization of a thin film ZrN diffusion barrier in an As-fabricated U–7Mo/Al matrix dispersion fuel plate, J. of Nucl. Mater. 458 (2015) 406–418.

[9] BHATTACHARYA S., JAMISON L., SEIDMAN D.N., MOHAMED W., BEI Y., PELLIN M.J., YACOUT A.M., Nanocrystalline ZrN thin film development via atomic layer deposition for U-Mo powder. J. of Nucl. Mater. 526 (2019) 151-770.

[10] LU F., HUANG M., YAQOOB F., LANG M., NAMAVAR F., TRAUTMANN C., SUN H., EWING R.C. AND LIAN J., Displacive radiation-induced structural contraction in nanocrystalline ZrN, App. Phys. Lett. 101 (2012) 041904.

[11] JANSE VAN VUUREN A., SKURATOV V.A., UGLOV V.V., NEETHLING J.H., ZLOTSKI S.V., Radiation tolerance of nanostructured ZrN coatings against swift heavy ion irradiation. J. Nucl. Mater. 442 (2013)507–511.

[12] ALIYU A., SRIVASTAVA C., Correlation between growth texture, crystallite size, lattice strain and corrosion behavior of copper-carbon nanotube composite coatings, Surface & Coatings Technology 405 (2021) 126596.

[13] ALSHAMSI A. S. AND ALBLOOSHI A., Effect of surface roughness on the corrosion behavior of pure iron in acidic solutions Int. J. Electrochem. Sci 14 (2019) 5794–5812.

[14] JANSE VAN VUUREN A., SKURATOV V.A., UGLOV V.V., NEETHLING J.H., ZLOTSKI S.V., Radiation tolerance of nanostructured ZrN coatings against swift heavy ion irradiation. J. Nucl. Mater. 442 (2013)507–511.

[15] HAGHSHENAS M., KLASSEN R.J., LIU S.F., Depth-sensing cyclic nanoindentation of Tantalum. International Journal of Refractory Metals and Hard Materials. 66 (2017) 144-149.

[16] KEISER D.D., PEREZ E., WIENCEK T., LEENAERS A., VAN DEN BERGHE S. (2015)Microstructural characterization of a thin film ZrN diffusion barrier in an As-fabricated U–7Mo/Al matrix dispersion fuel plate, J. of Nucl. Mater. 458, 406–418.